Chemistry Faculty Publications

Chemistry

4-2003

Peptide-protein Interactions: Photoinduced Electron-transfer Within The Preformed And Encounter Complexes Of A Designed Metallopeptide And Cytochrome C

Robin C. Lasey

Liu Liu

Ling Zang

Michael Y. Ogawa
Bowling Green State University - Main Campus, mogawa@bgsu.edu

Follow this and additional works at: http://scholarworks.bgsu.edu/chem_pub

Part of the Chemistry Commons

Peptide−Protein Interactions: Photoinduced Electron-Transfer within the Preformed and Encounter Complexes of a Designed Metallopeptide and Cytochrome *c*[†]

Robin C. Lasey, Liu Liu, Ling Zang, and Michael Y. Ogawa*

Department of Chemistry and Center for Photochemical Sciences, Bowling Green State University, Bowling Green, Ohio 43403

Received October 23, 2002; Revised Manuscript Received January 28, 2003

ABSTRACT: Photoinduced electron-transfer (ET) occurs between a negatively charged metallopeptide, [Ru(bpy)$_2$(phen-am)-Cys-(Glu)$_5$-Gly]$^{3-}$ = RuCE$_5$G, and ferricytochrome *c* = Cyt *c*. In the presence of Cyt *c*, the triplet state lifetime of the ruthenium metallopeptide is shortened, and the emission decays via biexponential kinetics, which indicates the existence of two excited-state populations of ruthenium peptides. The faster decay component displays concentration-independent kinetics demonstrating the presence of a preformed peptide−protein complex that undergoes intra-complex electron-transfer. Values of $K_b = (3.5 \pm 0.2) \times 10^4$ M^{-1} and $k_{ET}^{obs} = (2.7 \pm 0.4) \times 10^6$ s^{-1} were observed at ambient temperatures. The magnitude of k_{ET}^{obs} decreases with increasing solvent viscosity, and the behavior can be fit to the expression $k_{ET}^{obs} \propto \eta^{-\alpha}$ to give $\alpha = 0.59 \pm 0.05$. The electron-transfer process occurring in the preformed complex is therefore gated by a rate-limiting configurational change of the complex. The slower decay component displays concentration-dependent kinetics that saturate at high concentrations of Cyt *c*. Analysis according to rapid equilibrium formation of an encounter complex that undergoes unimolecular electron-transfer yields $K_b' = (2.5 \pm 0.7) \times 10^4$ M^{-1} and $k_{ET}^{obs'} = (7 \pm 3) \times 10^5$ s^{-1}. The different values of k_{ET}^{obs} and $k_{ET}^{obs'}$ suggest that the peptide lies farther from the heme when in the encounter complex. The value of $k_{ET}^{obs'}$ is viscosity dependent indicating that the reaction occurring within the encounter complex is also configurationally gated. A value of $\alpha = 0.98 \pm 0.14$ is observed for $k_{ET}^{obs'}$, which suggests that the rate-limiting gating processes in the encounter complex is different from that in the preformed complex.

Protein−protein interactions play fundamental roles in controlling the mechanisms of such important biological processes as gene regulation, enzyme inhibition, and protein self-assembly. Electron-transfer (ET) reactions can be used to probe the nature of these interactions in cases where the interacting proteins are known to be redox active. As much is now known about the factors that control the rates of long-range electron-transfers (*1*, *2*), ET studies can be used to provide detailed information about the way metalloproteins interact with one another, the stoichiometry of protein complexes, and the distances between the redox sites at the time of the reaction. A few of the many examples of this approach include early work in which the pH and ionic strength dependence of intermolecular ET rates involving cytochromes *c* and *b*$_5$ were used to support the electrostatic nature of their complex (*3*, *4*) as first proposed by Saleme (*5*). Later studies by Kostic and Qin examined the ET properties of covalently cross-linked protein complexes involving both physiological (*6*) and nonphysiological partners (*7*) to begin understanding how the dynamic nature of noncovalent protein complexes (*8−12*) significantly affects their redox reactivity. In other work, Hoffman and co-

workers (*13−16*) studied the concentration dependence of inter-protein ET rates to demonstrate the conformational heterogeneity of protein complexes. Here, cytochrome *c* peroxidase was shown to possess two separate binding sites for Cyt *c*, and the ET reaction involving the lower affinity site occurred at a faster rate than that from the higher affinity site. These workers have also defined a new dynamic docking paradigm for ET (*17*, *18*) in which interprotein interactions can involve numerous weakly bound conformations, of which only a small subset are ET active.

In this paper, a small, negatively charged metallopeptide is used to interact with the positively charged surface of ferricytochrome *c* (Cyt *c*)[1] to provide a simple model for more complicated protein−protein interactions (Figure 1). The designed peptide, RuCE$_5$G, contains a photoactive ruthenium polypyridyl complex that can undergo photo-induced electron-transfer to the iron(III) heme. It is shown that in the presence of Cyt *c*, the population of ruthenium

---

[1] Abbreviations: Cyt *c*, ferricytochrome *c*; Pc, plastocyanin; CcP, cytochrome *c* peroxidase; bpy, 2,2′-bipyridine; phen-AcCl, 5-chloro-acetamido-1,10-phenanthroline; phen-am, 5-acetamido-1,10-phenan-throline; Cys, cysteine; Glu, glutamic acid; Gly, glycine; k_{ET}, electron-transfer rate constant; NMP, *N*-methylpyrrolidone; HBTU, 2-(1H-benzotriazol-1-yl)-1,1,3,3-tetramethyluronium hexafluorophosphate; HOBT, 1-hydroxybenzotriazole; DIEA, *N,N*-diisopropylethylamine; DMF, *N,N*-dimethylformamide; HTFA, trifluoroacetic acid; TCEP, tris-(2-carboxyethyl)phosphine.
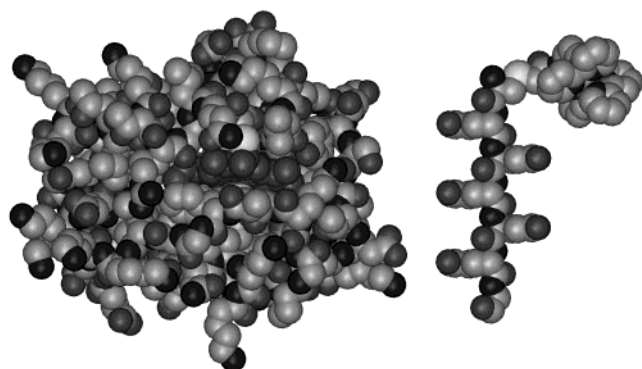

FIGURE 1: Computer models of cytochrome *c* and the $[Ru(CE_5G)]^{3-}$ metallopeptide.

excited states is quenched by a process that involves both a preformed peptide−protein complex and a transient excited-state encounter complex. The rate constants for these two distinct processes are compared, and it is suggested that the peptide probe interacts with different regions of the protein surface when it exists within these two complexes. It is further shown that the rates of electron-transfer occurring within both the encounter and the preformed complexes are gated by a rate determining configurational change of the complex. Comparison of the viscosity dependence of these rates suggests that the rate-limiting gating processes are different in the two complexes.

EXPERIMENTAL PROCEDURES

Materials. The Fmoc-protected L-amino acid derivatives, NMP, HBTU, piperidine, and HOBT were purchased from Peptides International, Inc. (Louisville, KY) and PE Biosystems (Foster City, CA). Dichloromethane, β-mercaptoethanol, HTFA, and phosphate buffer (50 mM pH 7.0) were obtained from Fisher Scientific (Pittsburgh, PA). Phenol was obtained from Aldrich Chemicals (Milwaukee, WI), and triisopropylsilane was from Lancaster Chemicals (Windham, NH). $Ru(bpy)_2(phen-AcCl)(PF_6)_2$, where bpy = 2,2′-bipyridine and phen-AcCl = 5-chloroacetamido-1,10-phenanthroline, was prepared as previously described (*19, 20*). Ferricytochrome *c* (Cyt *c*) from horse heart was purchased from Sigma (St. Louis, MO) and used as received. The amount of reduced metalloprotein ($\epsilon_{550} = 2.77 \times 10^4$ M^{-1} cm^{-1}) (*21*) in the sample was determined by converting it to the oxidized form ($\epsilon_{530} = 1.01 \times 10^4$ M^{-1} cm^{-1}) (*22*) with $K_3Fe(CN)_6$ and measuring the change in the absorption spectrum. The results showed that the Cyt *c* samples contained <3% of the reduced form.

Viscosity. Sucrose and phosphate buffer were combined to prepare solutions of various viscosities, as determined from tables (*23*). Care was taken to maintain a constant phosphate buffer concentration of 0.5 mM and pH 7 for all solutions.

General Methods. Reverse-phase HPLC runs were performed on either an Agilent Technologies semipreparative (9.4 × 250 mm) or preparative (21.2 × 250 mm) Zorbax 300SB-C18 column. A two-pump system (Waters Model 515) equipped with a Waters Model 996 diode array detector/spectrophotometer having a 1-cm path length cell was used. Linear gradients of acetonitrile and water, each containing 0.1% (v/v) trifluoroacetic acid, were used as the mobile phase. Absorption spectra were recorded on a Hewlett-

Packard 8452A spectrophotometer. Static luminescence spectra were obtained with a single photon counting spectrofluorimeter from Edinburgh Analytical Instruments (FL/FS 900). Electrospray ionization mass spectrometry was performed at the University of Cincinnati Mass Spectrometry Facility, Cincinnati, OH.

Synthesis of Ru(bpy)_2(phen-am)-Cys-(Glu)_5-Gly. The 7-residue oligopeptide Cys-(Glu)$_5$-Gly was synthesized on a PE Biosystems (Foster City, CA) model 433A peptide synthesizer using the Fmoc N-terminal protection strategy and the manufacturer's Fmoc-Gly-HMP resin. Activation was achieved using HBTU/HOBT in DMF. After the synthesis was complete, the resin-bound peptide was removed from the synthesizer and dried under vacuum overnight. The peptide was then separated from the resin by reaction with a cleavage cocktail comprised of trifluoroacetic acid (86% (v/v)), phenol (5% (v/v)), triisopropylsilane (2% (v/v)), β-mercaptoethanol (2% (v/v)), and water (5% (v/v)) for 2 h. The solution containing the resin and crude peptide was then filtered through glass wool, and the filtrate was added dropwise to cold diethyl ether set in a dry ice−acetone bath. The white precipitate was then collected by vacuum filtration, washed five times with diethyl ether, lyophilized, and used without further purification.

The synthesis of the $Ru(bpy)_2(phen-am)$-Cys-(Glu)$_5$-Gly metallopeptide, called RuCE$_5$G, was achieved by appropriate modification of methods described previously (*19*). In a typical preparation, 0.12 g of the CE$_5$G apopeptide was suspended in 50 mM phosphate buffer (pH 7), and 1 M NaOH(aq) was added dropwise until the peptide had completely dissolved. To this was added 0.24 g of TCEP, and the solution was stirred for 15 min. The pH was neutralized by the dropwise addition of NaOH(aq), and 0.1 g of $Ru(bpy)_2(phen-AcCl)(PF_6)_2$ was dissolved in a minimum amount of DMF and added to the reaction mixture. The resulting solution was stirred in the dark for about 24 h. The crude reaction products were purified by reverse-phase HPLC and analyzed by electrospray ionization mass spectrometry.

Emission Lifetime Measurements. Emission lifetimes were measured with a nitrogen-pumped broadband dye laser (2−3 nm fwhm). The excitation wavelength was set to 458 nm using Coumarin 460 (440−480 nm) dye, and the ruthenium emission was monitored at 610 nm. Unless otherwise noted, measurements were performed on argon-saturated solutions of the metallopeptide and Cyt *c* dissolved in low ionic strength phosphate buffer solution (typically 0.5 mM). The concentration of stock solutions of the RuCE$_5$G peptide (ca. 30 µM in water) and Cyt *c* (ca. 1 mM protein dissolved in either 5 or 10 mM phospate buffer) were determined by UV−vis spectroscopy using values of $\epsilon_{450} = 16,600$ M^{-1}cm^{-1} for the ruthenium polypyridyl center of the metallopeptide (*19*) and $\epsilon_{530} = 1.01 \times 10^4$ M^{-1}cm^{-1} for cytochrome *c* (*22*). Errors in electron-transfer rate constants and binding constants are expressed as 2σ.

RESULTS AND DISCUSSION

Characterization of the RuCE_5G Metallopeptide. The heptapeptide NH$_2$-Cys-(Glu)$_5$-Gly-OH was synthesized by solid-phase methods, and the cysteine side chain was alkylated by reaction with a ruthenium polypyridyl complex containing a chloroacetyl linker, $Ru(bpy)_2(phen-AcCl)^{2+}$,

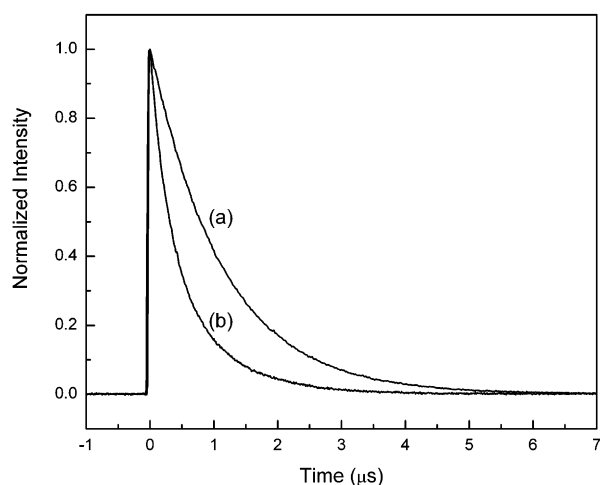FIGURE 2: Triplet decay traces of 7.0 μM RuCE$_5$G in the (a) absence and (b) presence of 40 μM Cyt c in argon-saturated 0.5 mM phosphate buffer solutions at pH 7. The traces are fit to monoexponential and double-exponential kinetics, respectively. For comparison, the intensities are normalized at time zero.

FIGURE 3: Magnitudes of k_S and k_L as a function of total Cyt c concentration in 0.5 mM phosphate buffer, pH 7. Error bars indicate uncertainty in the results of the fits of the lifetime data to eq 2.

using methods described previously (*19*). The resulting metallopeptide, designated RuCE$_5$G, was purified by preparative reversed-phase HPLC, and its identity was confirmed by electrospray ionization mass spectrometry (*m/z*: [M]$^+$ calcd for RuCE$_5$G, 1473.0; found, 1472.6; [M]$^{2+}$ calcd for RuCE$_5$G, 736.5; found, 736.2).

The UV−vis absorption spectra of RuCE$_5$G and its Ru(bpy)$_2$(phen-AcCl) starting material are very similar to one another. Both display MLCT bands centered at 450 nm indicating that the electronic structure of the ruthenium polypyridyl complex remains unchanged upon attachment to the peptide. The emission of the two ruthenium complexes are also very similar, with maxima occurring at 610 nm and decays that follow single-exponential kinetics. At 298 K, pH 7.0 the emission of RuCE$_5$G decays with a first-order rate constant of $k_0 = (8.93 \pm 0.08) \times 10^5$ s^{-1} when measured in argon-saturated aqueous solution (Figure 2).

The emission lifetime of RuCE$_5$G decreases with increasing temperature within the range of 276−330 K (not shown). This behavior can be accurately fit to eq 1 which has been used to describe the temperature-dependent emission lifetimes of numerous ruthenium polypyridyl compounds as arising from a deactivation process that involves the thermal population of higher energy d−d states (*24−26*).

$$k_0 = 1/\tau_0 = [(k_r + k_{nr}) + k_t \exp(-E_a/RT)] \quad (1)$$

In this expression k_r and k_{nr} refer, respectively, to the nominally temperature-independent rate constants for the radiative and nonradiative emission decay processes, and k_t refers to the dominant temperature-dependent decay mechanism having activation energy E_a. A fit of the data to eq 1 yields values of $(k_r + k_{nr}) = (6.1 \pm 0.1) \times 10^5$ s^{-1}, $k_t = (2.1 \pm 0.5) \times 10^{13}$ s^{-1}, and $E_a = 3740 \pm 60$ cm^{-1}, which are typical for related compounds (*24, 26*).

Effect of Cyt c on the Triplet Decay Kinetics of RuCE$_5$G. The emission lifetime of RuCE$_5$G is shortened and decays via biexponential kinetics in the presence of Cyt c (Figure 2). Transient absorption spectroscopy shows that this behavior is accompanied by an increased intensity of the absorption band at 550 nm arising from the reduced form of
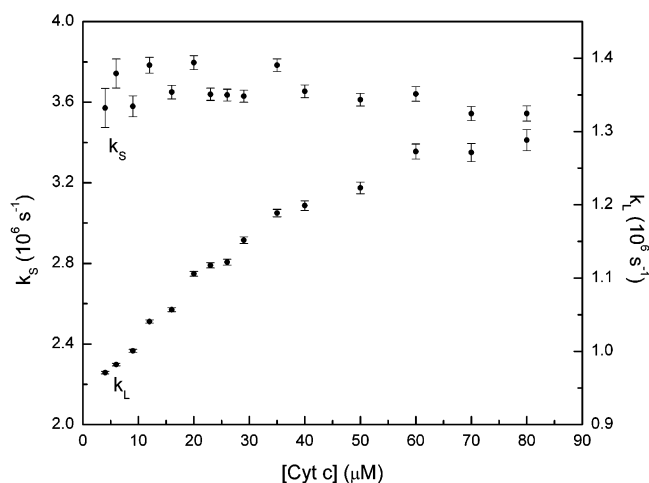
Cyt c. Taken in concert, these results are similar to those of Turro et al. (*27*) who demonstrated that Cyt c quenches the luminescence of several ruthenium polypyridyl compounds exclusively by photoinduced electron-transfer.

The emission decay measured from solutions containing both RuCE$_5$G and Cyt c can be accurately fit to double exponential decay kinetics (eq 2)

$$I(t) = A_S \exp(-k_S t) + A_L \exp(-k_L t) \quad (2)$$

in which A_S, k_S and A_L, k_L are the amplitudes and rate constants of the shorter and longer lifetime components, respectively. As the concentration of Cyt c in solution is increased from ca. 1 to 80 μM the magnitude of k_S remains constant, having a mean value of $k_S = (3.6 \pm 0.1) \times 10^6$ s^{-1}. However, it is also seen that the fractional population of the shorter lived species increases with increasing concentration of Cyt c. The magnitude of k_L also varies with protein concentration and approaches a saturating value at concentrations above 60 μM (Figure 3). Together, these results indicate that two kinetically distinct populations of photoexcited [RuCE$_5$G]* peptides exist in the presence of Cyt c and that these populations do not rapidly interconvert on the time scale of the experiment. As will be shown below, one population exists within a preformed peptide−protein complex in which the emission of [RuCE$_5$G]* is quenched by an intracomplex ET reaction having rate constant k_{ET}^{obs}, and the remaining population undergoes the diffusional formation of an excited-state encounter complex within which ET proceeds with the unimolecular rate constant $k_{ET}^{obs'}$. Similar schemes have been used to describe the photoinduced electron-transfer behavior in aqueous solutions of zinc-substituted Cyt c and cupriplastocyanin (*8−11*) and for those of Cyt c and negatively charged zinc porphyrins (*28, 29*).

Preformed Complex. The relative amplitudes of the two decay components, A_S and A_L, can be used to determine the fraction of ruthenium peptides that exist within the preformed complex according to eq 3.

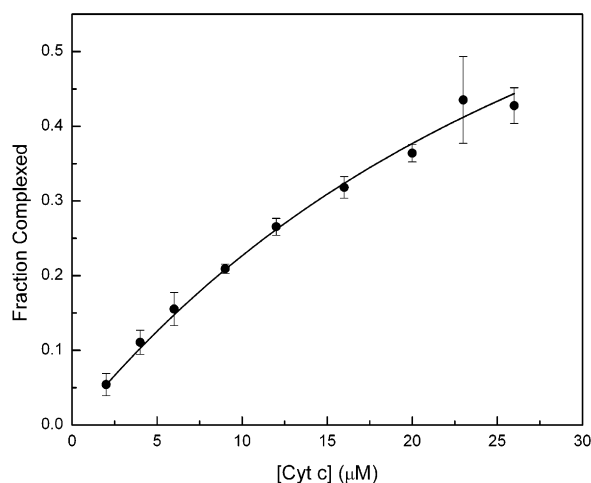$$f_{complexed} = (A_S)/(A_S + A_L) \quad (3)$$

FIGURE 4: Fraction of the RuCE$_5$G species existing in the preformed complex as a function of total Cyt *c* concentration. The solid line represents the fit to the 1:1 binding isotherm (eq 4). The total concentration of RuCE$_5$G is 7.0 μM in 0.5 mM phosphate buffer, pH 7. The error bars reflect the standard deviation of results obtained from the average of three independent experiments.

Figure 4 shows that the values of $f_{complexed}$ increase with increasing [Cyt *c*] and can be accurately described by the 1:1 binding isotherm (eq 4) within the concentration range examined. In eq 4, K_b is the equilibrium binding constant, and [Ru]$_0$ = 7.0 μM is the initial concentration of RuCE$_5$G. The solid line shows the results of a nonlinear least-squares fit of the data to eq 4. The results at 298 K give a binding constant of $K_b = (3.5 \pm 0.2) \times 10^4$ M^{-1} in 0.5 mM phosphate buffer at pH 7.

$$f_{complexed} =$$

$$\frac{1/K_b + [\text{Ru}]_0 + [\text{Cyt } c] - \sqrt{(1/K_b + [\text{Ru}]_0 + [\text{Cyt } c])^2 - 4[\text{Ru}]_0[\text{Cyt}c]}}{2[\text{Ru}]_0}$$

$$(4)$$

Variation of buffer concentration shows that the magnitude of K_b decreases with increasing ionic strength, demonstrating that the preformed peptide−protein complex is electrostatic in nature.

To obtain the thermodynamic parameters for the formation of the RuCE$_5$G/Cyt *c* complex, the values of K_b were determined at different temperatures according to eq 4 using values of $f_{complexed}$ observed for solutions having [RuCE$_5$G]$_0$ = 7.0 μM and [Cyt *c*] = 14.0 μM. Figure 5 shows that the values of K_b increase with increasing temperature and yield a linear van't Hoff plot (ln K_b vs $1/T$) to give values of ΔS_{bind} = +119 $\pm$ 3 J mol^{-1} K^{-1} and ΔH_{bind} = 10.3 $\pm$ 0.8 kJ mol^{-1}. These results show that the formation of the peptide−protein complex is entropy-controlled and suggests that the assembly process is driven by the release of surface bound water molecules (*30*). The desolvation process apparently carries a significant enthalpic cost that results in an overall positive ΔH_{bind} despite the electrostatic attraction occurring between RuCE$_5$G and Cyt *c* (*31*). Indeed, small positive values of ΔH_{bind} and large positive values of ΔS_{bind} have been previously observed for the formation of electrostatic protein−protein complexes (*12, 32, 33*).

Kinetics of ET within the Preformed Complex. Figure 3 shows that the lifetime of the shorter decay component is independent of Cyt *c* concentration, which indicates that a
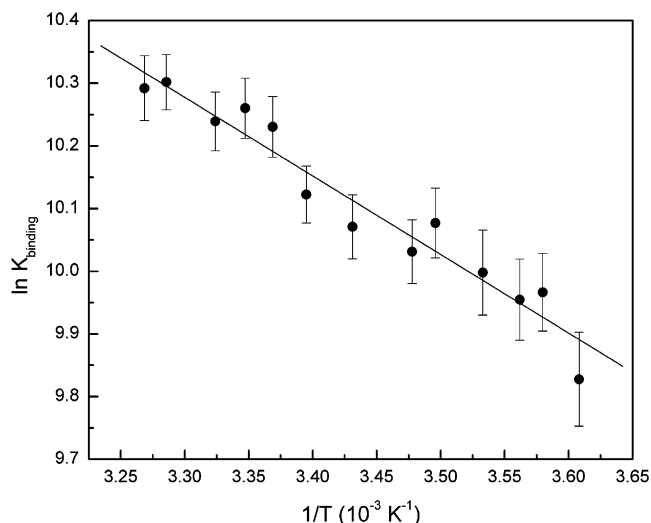

FIGURE 5: Temperature dependence of K_b for the preformed complex between RuCE$_5$G and Cyt *c*. Conditions: [RuCE$_5$G] = 7 μM, [Cyt *c*] = 14 μM in 0.5 mM phosphate buffer, pH 7. Error bars are from the uncertainty in the results of the fits of the lifetime data to eq 2.

unimolecular electron-transfer reaction occurs within the preformed peptide−protein complex. The apparent intracomplex ET rate constant is calculated to be $k_{ET}^{obs} = (k_S - k_0) = (2.7 \pm 0.4) \times 10^6$ s^{-1}, where k_0 is the decay rate constant measured in the absence of Cyt *c*.

The temperature dependence of k_{ET}^{obs} was analyzed according to the Eyring equation (eq 5)

$$k_{ET}^{obs} = \left(\frac{k_B T}{h}\right) \exp\left(\frac{\Delta S^{\ddagger}}{R}\right) \exp\left(\frac{-\Delta H^{\ddagger}}{RT}\right) \qquad (5)$$

to yield the activation parameters for the intracomplex electron-transfer reaction, where k_B is Boltzmann's constant, h is Planck's constant, $\Delta S^{\ddagger}$ is the activation entropy, and $\Delta H^{\ddagger}$ is the activation enthalpy. The data yield values of $\Delta S^{\ddagger}$ = −78 $\pm$ 6 J K^{-1} mol^{-1} and $\Delta H^{\ddagger}$ = 13 $\pm$ 2 kJ mol^{-1}. The values of both $\Delta S^{\ddagger}$ and $\Delta H^{\ddagger}$ obtained for RuCE$_5$G/Cyt *c* are consistent, in both amplitude and sign, with those reported by Harris and Davidson (*34*) and Ivkovic-Jensen and Kostic (*12*) for intracomplex ET reactions occurring in the Cyt *c*/Cyt *c* peroxidase and Cyt *c*/plastocyanin systems, respectively. The negative activation entropy suggests that formation of the transition state requires a reorientation of the preformed peptide−protein complex prior to the electron-transfer event. Support for this hypothesis can be seen in Figure 6, which shows how the observed intracomplex electron-transfer rate constant, k_{ET}^{obs}, depends on solvent viscosity. Solutions were prepared by mixing differing amounts of sucrose and phosphate buffer in such a way as to maintain a constant pH and ionic strength. Under these conditions, the emission of the RuCE$_5$G peptide was seen to decay by a sum of two exponentials, as described above for experiments performed in the absence of viscogen (eq 2). Further, the relative amplitudes of the slow and fast decay components were seen to be independent of sucrose concentration, which indicates that the addition of sucrose does not affect the binding interactions within the preformed complex. As shown in Figure 6, the values of k_{ET}^{obs} decrease smoothly with increasing viscosity and were fit to an empirical exponential

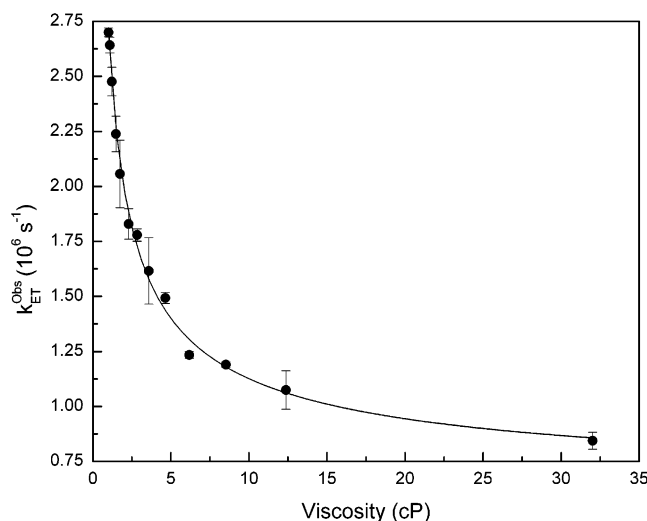FIGURE 6: Viscosity dependence of k_{ET}^{obs}, the rate constant for electron-transfer occurring within the preformed complex. The solid line represents a fit of the data to eq 6 as described in the text. The error bars reflect the standard deviation of results obtained from the average of two independent experiments performed for each point.

FIGURE 7: Observed rate constants (k_L) of the slower component of the triplet decay of RuCE$_5$G (7.0 μM) as a function of the concentration of free (i.e., uncomplexed) Cyt c. The solid line represents the fit of the data to eq 9. Conditions: argon-saturated, 0.5 mM, pH 7 phosphate buffer solutions at 297 K. The error bars reflect the standard deviation of results obtained from the average of three independent experiments performed for each point.

relationship (eq 6) to yield values of $A = (2.10 \pm 0.09) \times 10^6$ s^{-1}, $C = (5.9 \pm 0.9) \times 10^5$ s^{-1}, and $\alpha = 0.59 \pm 0.05$. The value obtained for the exponent is lower in magnitude than the value of $\alpha = 1$ predicted by Kramers' theory (*35*) but comparable to those observed for some related protein−protein studies for which values of α have been reported to be in the range of 0.6−0.7 (*36, 37*).

$$k_{ET}^{obs} = A\eta^{-\alpha} + C \qquad (6)$$

The viscosity experiments show that the values obtained for k_{ET}^{obs} do not reflect the rates of a true ET event, but rather, are determined by the rates of a slow conformational gating process: $k_{ET}^{obs} = k_{gate} < k_{ET}^{true}$ (*38−40*). Thus, the values of k_{ET}^{obs} provide a lower limit for k_{ET}^{true}. In turn, this can be used to estimate an upper limit for the donor−acceptor distance in the preformed complex according to eq 7

$$k_{ET}^{obs} = k_0 \exp[-\beta(r - r_0)] \exp\left[\frac{-(\Delta G^0 + \lambda)^2}{4\lambda RT}\right] \quad (7)$$

in which k_{ET}^{obs} is the value obtained at lowest viscosity, $k_0 = 10^{13}$ s^{-1}, β is the distance attenuation factor taken to be $\beta = 1.2$ Å^{-1}, r is the donor−acceptor separation, r_0 is the van der Waals contact distance of the reactants, and λ is the reorganization barrier (*41*). A value of $\Delta G^0 = -1.08$ eV is calculated from eq 8 (*24*)

$$\Delta G^0 = -E^{00} + E^0(Ru^{III}/Ru^{II}) - E^0(Cytc^{III}/Cytc^{II}) \quad (8)$$

where $E^{00} = 2.14$ eV is the triplet energy of RuCE$_5$G as determined from its emission spectrum measured at 77 K, $E^0(Ru^{III}/Ru^{II}) = 1.32$ V (*20*), and $E^0(Cyt\ c^{III}/Cyt\ c^{II}) = 0.26$ V (*42*). Assuming $\lambda = 0.8$ eV, as estimated for Ru(bpy)$_3$ and Cyt c (*43*), eq 7 yields an estimated donor−acceptor separation of $r < 15$ Å within the preformed complex.

ET Kinetics in the Encounter Complex. At protein concentrations below 6 μM, the slower decay component (k_L) of the triplet state of the RuCE$_5$G varies linearly with the
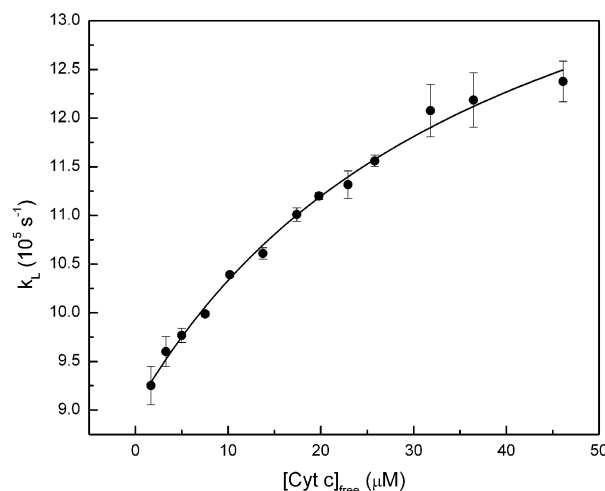
concentration of free Cyt c, [Cyt c]$_{free}$, to give a bimolecular electron-transfer rate constant of $k_{bi} = (k_L - k_0)/[\text{Cyt } c]_{free} = 1.5 \times 10^{10}$ M^{-1} s^{-1} at ambient temperature. The values of k_{bi} decrease with increasing ionic strength, demonstrating the role of electrostatic interactions on the formation of the peptide−protein encounter complex. It is noted that the ionic strength dependence of k_{bi} is significantly lower than that for K_b (not shown), which suggests that the collisional encounter between RuCE$_5$G and Cyt c experiences a substantially smaller effective charge product (Z_1Z_2) than in the preformed complex.

Figure 7 shows that when the concentration of the free Cyt c is raised above 6 μM, the values of k_L begin to saturate, indicating the formation of an excited-state encounter complex. According to Scheme 1, the kinetics of this bimolecular ET reaction can be described by eq 9

$$k_L = k_0 + \frac{k_{ET}^{obs'} K_b'[\text{Cyt } c]_{free}}{1 + K_b'[\text{Cyt } c]_{free}} \qquad (9)$$

which assumes a rapid preequilibrium step, where k_0 is as previously described, $k_{ET}^{obs'}$ is the observed rate constant for electron-transfer occurring within the encounter complex, and K_b' is the binding constant for encounter complex formation, defined as $K_b' = k_{on}/k_{off}$ (*44, 45*). The data conform very well to eq 9 to give $k_0 = (9.0 \pm 0.1) \times 10^5$ s^{-1}, which agrees with the value of $k_0 = (8.93 \pm 0.08) \times 10^5$ s^{-1} directly obtained from the lifetime of metallopeptide alone as discussed above. The fit to eq 9 also yields values of $k_{ET}^{obs'} = (7 \pm 3) \times 10^5$ s^{-1} and $K_b' = (2.5 \pm 0.7) \times 10^4$ M^{-1} at ambient temperature. Application of the steady-state approximation to Scheme 1 yields poor fits to the lifetime behavior since the concentration of the excited-state intermediate is not constant but decays with time.

As seen in Table 1, the unimolecular rate constant for electron-transfer occurring within the transient encounter complex ($k_{ET}^{obs'}$) is 4-fold smaller than that observed for the reaction occurring within the preformed complex (k_{ET}^{obs})

Scheme 1

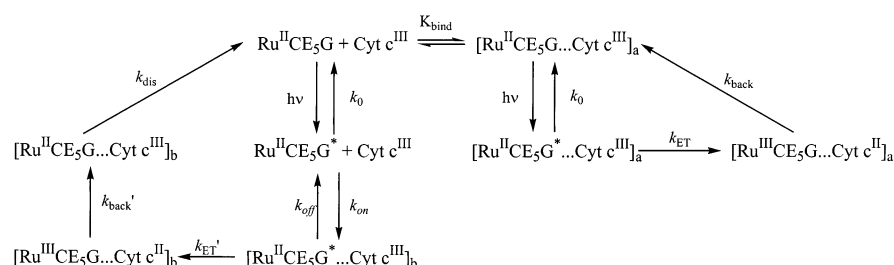Table 1: Comparison of ET Parameters and Binding Constants for Preformed and Encounter Complexes

	k_{ET}^{obs} (10^6 s^{-1})	K_b (10^4 M^{-1})	α
preformed complex	$(2.7 \pm 0.4)^{a,b}$	$3.5 \pm 0.2^{a,b}$	0.59 ± 0.05
encounter complex	$(0.7 \pm 0.3)^{a,b}$	$2.5 \pm 0.7^{a,b}$	0.98 ± 0.14

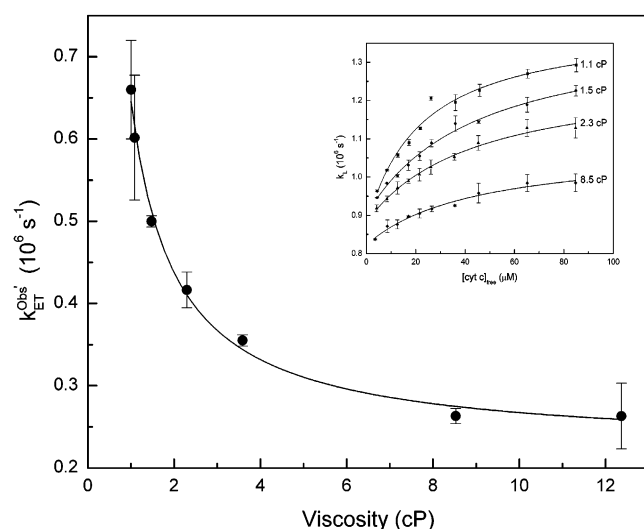[a] 0.5 mM phosphate buffer, pH 7, 297 K. [b] Errors are expressed as two standard deviations from the mean.

FIGURE 8: Viscosity dependence of $k_{ET}^{obs'}$, the rate constant for electron-transfer occurring within the transient encounter complex. The solid line represents a fit of the data to eq 6 as described in the text. The error bars reflect the standard deviation of results obtained from the average of two independent experiments performed for each point. Inset: Dependence of the long component of the triplet decay (k_L) on the concentration of free Cyt c obtained at different solution viscosities. The data obtained at 3.6 and 12.4 cP were omitted for clarity.

indicating that the encounter complex has a slightly longer (ca. 1 Å) donor−acceptor separation. The activation parameters for the ET reaction occurring in the encounter complex are $\Delta H^\ddagger = 10 \pm 1$ kJ mol^{-1} and $\Delta S^\ddagger = -100 \pm 4$ J K^{-1} mol^{-1}.

The concentration dependence of k_L was also determined using buffers containing 4, 14, 24, 32, 44, and 48% sucrose by weight, for which $\eta = 1.1$, 1.5, 2.3, 3.6, 8.5, and 12.4 cP, respectively. In all cases, the behavior could be accurately fit to eq 9 (inset, Figure 8) giving values of K_b' that remain constant within experimental error and values of $k_{ET}^{obs'}$ that decrease with increasing viscosity. Thus, the ET event occurring within the encounter complex is also gated by a rate-limiting configurational change of the complex. Figure 8 shows that the viscosity dependence of $k_{ET}^{obs'}$ can be

described by eq 6 in which a nonlinear least-squares fit yields values of $A = (4.2 \pm 0.2) \times 10^5$ s^{-1}, $C = (2.2 \pm 0.2) \times 10^5$ s^{-1}, and $\alpha = 0.98 \pm 0.14$.

CONCLUSIONS

A simple ruthenium metallopeptide (RuCE$_5$G) has been designed that has been shown to form electrostatic complexes with cytochrome c through an entropy-driven process. The results of the emission lifetime experiments show that photoinduced electron-transfer can proceed between RuCE$_5$G and Cyt c through parallel pathways that involve either the formation of a preformed peptide−protein complex or an excited-state encounter complex (Scheme 1). These results are different from those reported for reactions occurring between a variety of anionic zinc porphyrins and Cyt c, where photoinduced electron-transfer was seen to occur either within a preformed electrostatic complex (46), or between freely diffusing redox partners (47), but is somewhat similar to that seen by Kostic and co-workers in solutions of the nonphysiological redox partners, zinc cytochrome c and cupriplastocyanin. However, whereas in that system it was determined that the preformed and encounter complexes were conformationally identical (12), such does not appear to be the case for the peptide−protein complexes studied here. Rather, the results suggest that the initial encounter between photoexcited RuCE$_5$G and Cyt c appears to occur at a sterically accessible site of the protein surface from which unimolecular electron-transfer can occur. The observation of biexponential decay kinetics indicates that an additional, more persistent (i.e., preformed), peptide−protein complex also exists that can undergo intracomplex electron-transfer upon photoexcitation. The rate constants for these two intracomplex ET reactions are different. Viscosity experiments further show that the ET processes occurring in both the encounter and the persistent complexes are configurationally gated by motion of the peptide across the protein surface. Comparison of the viscosity dependence of k_{ET}^{obs} and $k_{ET}^{obs'}$ suggests that these motions differ in a manner that reflects the more dynamic nature of the encounter complex. Future work will investigate whether changes made to the metallopeptide sequence can selectively alter the gating processes occurring in either the preformed or the encounter peptide−protein complexes in this system.

REFERENCES

1. Winkler, J. R., and Gray, H. B. (1997) *J. Biol. Inorg. Chem. 2*, 399−404.

2. Page, C. C., Moser, C. C., Chen, X. X., and Dutton, P. L. (1999) *Nature 402*, 47−52.
3. Stonehuerner, J., Williams, J. B., and Millett, F. (1979) *Biochemistry 18*, 5422−5427.
4. Mauk, M. R., Reid, L. S., and Mauk, A. G. (1982) *Biochemistry 21*, 1843−1846.
5. Saleme, F. R. (1976) *J. Mol. Biol. 102*, 563−568.
6. Qin, L., and Kostic, N. M. (1993) *Biochemistry 32*, 6073−6080.
7. Qin, L., and Kostic, N. M. (1996) *Biochemistry 35*, 3379−3386.
8. Zhou, J. S., and Kostic, N. M. (1991) *J. Am. Chem. Soc. 113*, 6067−6073.
9. Zhou, J. S., and Kostic, N. M. (1992) *J. Am. Chem. Soc. 114*, 3562−3563.
10. Zhou, J. S., and Kostic, N. M. (1993) *J. Am. Chem. Soc. 115*, 10796−10804.
11. Zhou, J. S., and Kostic, N. M. (1993) *Biochemistry 32*, 4539−4546.
12. Ivkovic-Jensen, M. M., and Kostic, N. M. (1996) *Biochemistry 35*, 15095−15106.
13. Stemp, E. D. A., and Hoffman, B. M. (1993) *Biochemistry 32*, 10848−10865.
14. Zhou, J. S., and Hoffman, B. M. (1994) *Science 265*, 1693−1696.
15. Nocek, J. M., Zhou, J. S., DeForest, S., Priyadarshy, S., Beratan, D. N., Onuchic, J. N., and Hoffman, B. M. (1996) *Chem. Rev. 96*, 2459−2489.
16. Leesch, V. W., Bujons, J., Mauk, A. G., and Hoffman, B. M. (2000) *Biochemistry 39*, 10132−10139.
17. Liang, Z. X., Nocek, J. M., Huang, K., Hayes, R. T., Kurnikov, I. V., Beratan, D. N., and Hoffman, B. M. (2002) *J. Am. Chem. Soc. 124*, 6849−6859.
18. Liang, Z. X., Jiang, M., Ning, Q., and Hoffman, B. M. (2002) *J. Biol. Inorg. Chem. 7*, 580−588.
19. Fedorova, A., and Ogawa, M. Y. (2002) *Bioconjugate Chem. 13*, 150−154.
20. Fedorova, A., Chaudhari, A., and Ogawa, M. Y. (2003) *J. Am. Chem. Soc. 125*, 357−362.
21. Vanderkooi, J. M., Adar, F., and M., E. (1976) *Eur. J. Biochem. 64*, 381−387.
22. Wikstrom, M., Krab, K., and Saraste, M. (1981) *Cytochrome Oxidase: A Synthesis*, Academic Press, New York.
23. (1986) (West, R. C., Ed.), CRC Press, Boca Raton, FL.
24. Juris, A., Balzani, V., Barigelletti, F., Campagna, S., Belser, P., and Vonzelewsky, A. (1988) *Coord. Chem. Rev. 84*, 85−277.
25. Fernando, S. R. L., Maharoof, U. S. M., Deshayes, K. D., Kinstle, T. H., and Ogawa, M. Y. (1996) *J. Am. Chem. Soc. 118*, 5783−5790.
26. Kise, K. J., and Bowler, B. E. (2002) *Inorg. Chem. 41*, 379−386.
27. Turro, C., Zaleski, J. M., Karabatsos, Y. M., and Nocera, D. G. (1996) *J. Am. Chem. Soc. 118*, 6060−6067.
28. Croney, J. C., Helms, M. K., Jameson, D. M., and Larsen, R. W. (2000) *J. Phys. Chem. B 104*, 973−977.
29. Larsen, R. W., Omdal, D. H., Jasuja, R., Niu, S. L., and Jameson, D. M. (1997) *J. Phys. Chem. B 101*, 8012−8020.
30. Stites, W. E. (1997) *Chem. Rev. 97*, 1233−1250.
31. Sleigh, S. H., Seavers, P. R., Wilkinson, A. J., Ladbury, J. E., and Tame, J. R. H. (1999) *J. Mol. Biol. 291*, 393−415.
32. Mauk, M. R., Ferrer, J. C., and Mauk, A. G. (1994) *Biochemistry 33*, 12609−12614.
33. Kresheck, G. C., Vitello, L. B., and Erman, J. E. (1995) *Biochemistry 34*, 8398−8405.
34. Harris, T. K., and Davidson, V. L. (1993) *Biochemistry 32*, 14145−14150.
35. Kramers, H. A. (1940) *Physica 7*.
36. Qin, L., and Kostic, N. M. (1994) *Biochemistry 33*, 12592−12599.
37. Feng, C. J., Kedia, R. V., Hazzard, J. T., Hurley, J. K., Tollin, G., and Enemark, J. H. (2002) *Biochemistry 41*, 5816−5821.
38. Davidson, V. L. (2000) *Acc. Chem. Res. 33*, 87−93.
39. Hoffman, B. M., Ratner, M. A., and Wallin, S. A. (1990) *Adv. Chem. Ser.*, 125−146.
40. Hoffman, B. M., and Ratner, M. A. (1987) *J. Am. Chem. Soc. 109*, 6237−6243.
41. Marcus, R. A., and Sutin, N. (1985) *Biochim. Biophys. Acta 811*, 265−322.
42. Armstrong, G. D., Chambers, J. A., and Sykes, A. G. (1986) *J. Chem. Soc., Dalton Trans.*, 755−758.
43. Durham, B., Pan, L. P., Long, J. E., and Millett, F. (1989) *Biochemistry 28*, 8659−8665.
44. Harris, M. R., Davis, D. J., Durham, B., and Millett, F. (1997) *Biochim. Biophys. Acta 1319*, 147−154.
45. Peerey, L. M., and Kostic, N. M. (1989) *Biochemistry 28*, 1861−1868.
46. Zhou, J. S., Granada, E. S. V., Leontis, N. B., and Rodgers, M. A. J. (1990) *J. Am. Chem. Soc. 112*, 5074−5080.
47. Cho, K. C., Che, C. M., Ng, K. M., and Choy, C. L. (1986) *J. Am. Chem. Soc. 108*, 2814−2818.